Brain connectivity in patients with dystonia during motor tasks

Journal of Neural Engineering

PAPER

Brain connectivity in patients with dystonia during motor tasks

Carlos Arruda Baltazar[1], Birajara Soares Machado[1], Danilo Donizete de Faria[1,2,3], Artur José Marques Paulo[1], Sonia Maria Cezar Azevedo Silva[2,3], Henrique Ballalai Ferraz[2] and Patrícia de Carvalho Aguiar[1,2]

[1] Hospital Israelita Albert Einstein, Av. Albert Einstein 627, SP 05652–900, Brazil
[2] Escola Paulista de Medicina—UNIFESP, Department of Neurology and Neurosurgery, R. Pedro de Toledo 650, SP 04039–002, Brazil
[3] Hospital do Servidor Público Estadual de São Paulo, R. Pedro de Toledo 1800, SP 04039–000, Brazil

E-mail: carlos.baltazar@einstein.br, birajara.machado@einstein.br, birasm@gmail.com and patricia.aguiar@einstein.br

Keywords: dystonia, brain connectivity, complex networks, EEG

Supplementary material for this article is available online

OPEN ACCESS

RECEIVED
11 March 2020

REVISED
25 August 2020

ACCEPTED FOR PUBLICATION
25 September 2020

PUBLISHED
27 October 2020

Abstract

Objective. This study aims to investigate alterations of brain connectivity using multivariate electroencephalographic data to provide new insights of the brain connectivity dynamics of dystonia. *Approach*. We recorded electroencephalography (EEG) of patients with right upper limb idiopathic focal dystonia and paired controls during resting state, writing-from-memory, and finger-tapping tasks. We applied power spectrum analyses considering the mu, beta and gamma rhythms of the motor cortex and analyzed brain connectivity networks and microstates (MS). *Main results.* The power spectra results showed that patients had a loss of desynchronization of the beta rhythm during the writing task. We observed differences in the structure of the connective core in beta rhythm, as well as, in the intensity of the patient's hubs observed with basis in path length measures in mu and beta rhythms. Abnormalities were also identified in MS of default mode networks of patients associated with its performances during motor tasks. *Significance*. The EEG connectivity analyses provided interesting insights about the cortical electrophysiological patterns in dystonia, such as loss of event-related desynchronization, changes in the effective connectivity with similar signature to other neurological diseases, indications of alterations in the default-mode-network. Our findings are consistent with previously described connectivity abnormalities in neuroimaging studies confirming that dystonia is a network disorder.

1. Introduction

Dystonia is a neurological syndrome characterized by sustained involuntary muscle contractions, leading to repetitive twists and/or postural abnormalities (Albanese *et al* 2013). It is often triggered or worsened by voluntary action and associated with overflow of muscle activation. These patients present sensorimotor disturbances that lead to disability (Fahn *et al* 1998).

Among movement disorders, dystonia is one of the most complex in terms of its pathophysiology. It is widely associated with structural lesions in basal nuclei and thalamus, but idiopathic dystonia cases do not present any structural lesions. Three main hypotheses can explain the pathophysiology of this type of dystonia: loss of intracortical and surround inhibition, dysfunction of sensorimotor integration and maladaptive neuroplasticity (Neychev *et al* 2011).

All these mechanisms lead us to think of dystonia as a network-disorder. The concept of brain connectivity provides useful tools to project the relationships between brain sites (Dresel *et al* 2014, Gallea *et al* 2015, Zoons *et al* 2011). The causal mechanism of dystonia could be related to: (i) structural connectivity which is characterized by anatomic tracts linking brain regions (Koch *et al* 2002); (ii) functional connectivity, defined by statistical and temporal dependence between distinct and anatomically distant brain regions (Sporns 2011) and; (iii) effective connectivity, described by the influence of one brain site over another, reflecting a causal relationship (Friston 2011). In addition, the complex networks theory is applied to study and quantify

brain connectivity in dystonia (Jin *et al* 2011). This approach can provide parameters that allow us to better understand the functional and effective features between the network nodes, as well as to identify abnormal patterns in the network caused by neurological disorders (Lo *et al* 2010, Jeong 2004).

This study aimed to investigate the characteristics of brain connectivity dynamics in patients with focal upper limb idiopathic dystonia using multivariate electroencephalography (EEG) acquired during resting-state, writing-from-memory, and finger-tapping tasks. We hypothesize that patients present altered dynamics of effective brain connectivity, such as abnormal network centrality parameters, as well as alterations in the power spectra representations and microstates (MS) parameters.

2. Data and methods

2.1. Patients

This study was approved by the review boards of all participating institutions, and all subjects gave informed written consent. Neurologists with experience in movement disorders recruited subjects according to the following criteria: age between 18 and 60 years, both genders, right-handed (assessed by the Edinburgh Handedness Inventory), native Portuguese speakers with more than eight years of formal education. Our study involved twenty patients with right upper limb focal dystonia (being nine men and eleven women); where two patients had family history and only one presented task-specific dystonia; with a mean age of 43.3 years; a mean disease duration of 10.95 years) and twenty health volunteers (ten men, ten women with a mean age of 42.25 years).

The diagnosis of idiopathic focal dystonia was established according to the current consensus (Albanese *et al* 2013), and patients were assessed with the Burke-Fahn-Marsden dystonia rating scale (as seen in supplemental material, table S1 (stacks.iop.org/JNE/17/056039/mmedia)). Dystonia patients and controls were matched for age and education level. The exclusion criteria were the presence of uncontrolled metabolic disorders, cancer, history of other neurological diseases (apart from dystonia), head and upper limb trauma or surgery, use of drugs that might interfere with the EEG signal; use of botulinum toxin in the last three months.

2.2. EEG Data

The EEG data were acquired using a 32-channel set, with active electrodes from ActiCap and a LiveAmp amplifier (Brain Products, Gilching DE). The electrodes were placed according to the 10–20 international standard system, and impedance was kept between 10 and 20 kΩ. We recorded the data with the Brain Vision Recorder (Brain Products, Gilching DE) at 250 Hz of sampling rate and pre-processed it using the Brain Vision Analyzer software 2.1 (Brain Products, Gilching DE). The data were filtered with a band-pass filter (0.5–50 Hz) and a notch filter at 60 Hz.

Muscle and eye artifacts were removed using independent component analysis and a semiautomatic correction feature. The channels were referenced with their average value. Data were processed using the Brain Connectivity Toolbox (Rubinov and Sporns 2010) and a plugin for processing MS with EEGLab Toolbox (Poulsen *et al* 2018), both used in Mathworks MATLAB® 2018a software.

2.3. Tasks

EEG and video were recorded during resting-state, finger-tapping and writing-from-memory tasks, with the following parameters: 1 min of resting-state to characterize the basal neuronal activity looking at a black cross on a white background (Damoiseaux *et al* 2006); 2 min of writing-from-memory task, composed by four blocks of 30 s each followed by 30 s of rest (see figure 1(A)); subjects had to write repeatedly the same sentence. Also, we wanted to avoid sentences that could demand significant cognitive efforts, focusing on the neural correlates of the motor task. Therefore we chose the first sentence of the song Happy Birthday to You (*Parabéns para você*, in Portuguese), due to its universal knowledge. The finger-tapping task consisted of 12 blocks of 30 s interspersed by 30 s of rest, as illustrated in figure 1(B). This task was randomly alternated between right, left of both hands (four blocks each). Subjects had to tap each finger against the thumb, from the index to the little finger, as fast and accurately as possible (Witt *et al* 2008). They were videotaped during all tasks.

2.4. Measures

2.4.1. Power spectra

Power spectra analysis was calculated using normalized power spectra considering mu (μ—12 to 15 Hz), beta (β—15 to 25 Hz) and gamma (γ—25 to 50 Hz) rhythms. The filter order bandpass parameters were 60, 48 and 30 for μ, β and γ rhythms respectively (the same parameters were considered in zero-phase filter). We calculated the mean power spectra proposed by Machado *et al* (2012), of all electrodes placed on the sensorimotor cortex (Fc5, Fc6, Cz, C3, C4, T7, T8, Cp1, Cp2, Cp5 and Cp6), denoted by:

$$\overline{E}_{\omega} = \frac{\int_{\nu_s}^{\nu_e} |\tilde{f}(\nu)|^2 d\nu}{\int_{\nu_s}^{\nu_e} d\nu}, \qquad (1)$$

where $\tilde{f}(\nu)$ is the Fourier transform of the electrophysiological signal $f(t)$ in a determined frequency range $\omega = [\nu_s, \nu_e]$. As the Fourier transform is a global representation of the signal, we used the Welch estimator (Welch 1967) to avoid local spurious spectral signatures in EEG signal recorded during the task. So, to apply this estimator, we segmented the time series in windows with 3 s (750 points) of duration with

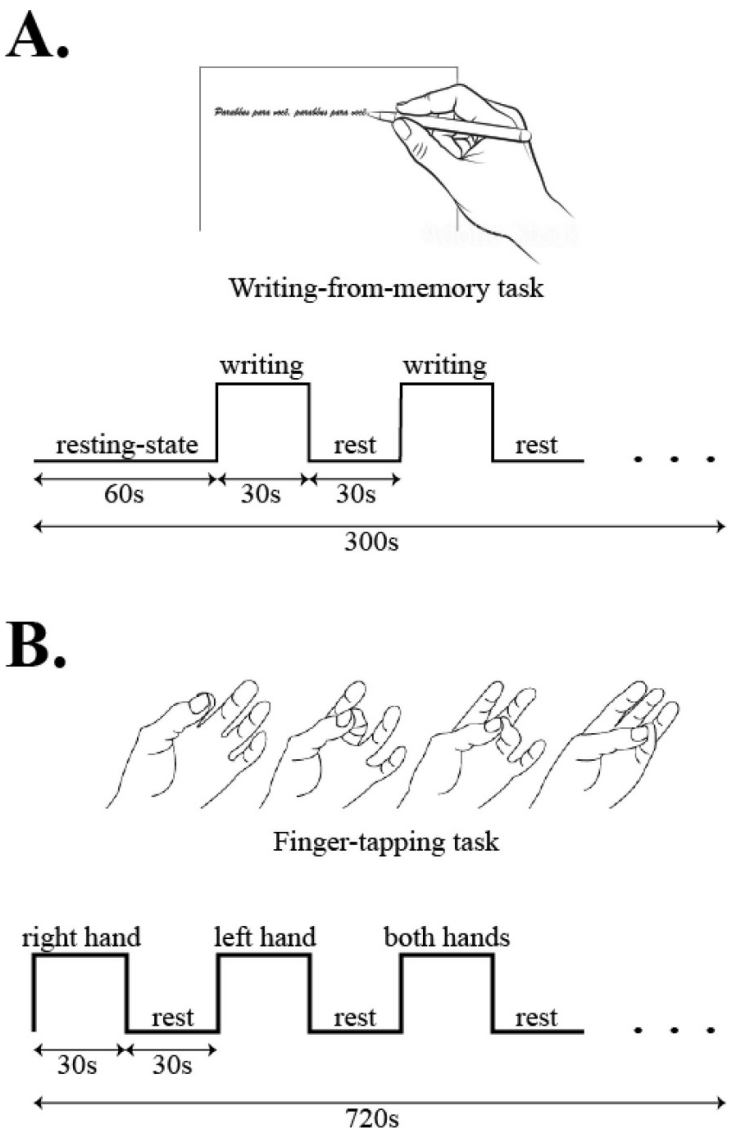

Figure 1. Schematic illustration of all tasks executed by subjects in this study: one minute of resting-state; four blocks of writing-from-memory task interspersed with rest periods (figure 1(A)) and twelve blocks of finger-tapping task, randomly anternating between right, left and both hands also interspersed with rest periods (figure 1(B)). All tasks illustared in this figure are described in details in section 2.3.

50% of overlap and calculated the mean power spectra of these segments to guarantee the signal stationarity (Machado *et al* 2012, Zhao and He 2013).

The μ-rhythm arises from the sensorimotor cortex during movement preparation and imagery. It originates from the synchronous activity of neurons in the thalamo-cortical loop and is physiologically attenuated by tactile stimuli or movement execution/imagery (event-related desynchronization) (Freeman *et al* 2016, Pfurtscheller *et al* 2006). The β-rhythm is also modulated in the sensorimotor cortex during the performance of voluntary movements (Jasper and Penfield 1949). Furthermore, γ-rhythm at sensorimotor cortex can be related to attentional process as a response to auditory stimuli, as well as, planning of voluntary movement and movement observation (Aoki *et al* 1999, Babiloni *et al* 2016).

Thus, to perform the power spectra analysis for each rhythm, we divided the sensorimotor cortex in the right and left hemispheres, that were compared within an individual and between individuals. The mean power of each rhythm is denoted by $\overline{E}_{\mu}$, $\overline{E}_{\beta}$ and $\overline{E}_{\gamma}$ for mu, beta and gamma rhythms, respectively (as illustrated in figure 2).

2.4.2. Normalized transfer entropy

To analyze the effective connectivity, we used a directional measure called normalized transfer entropy (*NTE*) proposed by Shovon *et al* (2014). *NTE* is an enhancement of the transfer entropy (*TE*) created by Schreiber (2000). *TE* incorporates non-linear, dynamic connections and their directional properties estimating if brain activity is dependent on another activity and not on its past. So, *TE* characterizes

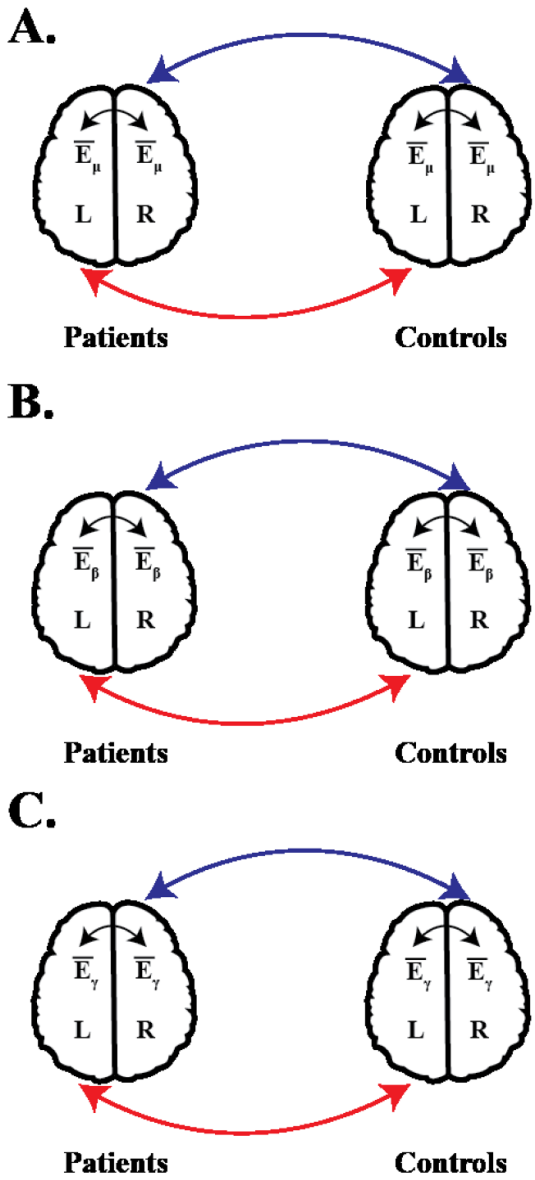

Figure 2. Schematic illustration of power spectra analysis of the mu (figure 2(A)), beta (figure 2(B)) and gamma (figure 2(C)) rhythms over the sensory-motor cortex (as described in section 2.4.1) during finger-tapping, resting-state and writing from memory tasks. We considered each hemisphere separately, so the left hemisphere was denoted by the letter 'L' and the right hemisphere was denoted by the letter 'R'. The black arrows represent the comparison of hemispheres within a individual, the red links represent the comparison of the left hemisphere between individuals and the blue links represent the comparison of the right hemisphere between individuals.

the information flow between two signals and is defined by:

$$TE_{Y\to X} = \sum_{t} p(x_{t+1}, x_t, y_t) \log_2 \frac{p(x_{t+1}|x_t, y_t)}{p(x_{t+1}|x_t)}, \quad (2)$$

where $p(x_{t+1}, x_t, y_t)$ is the joint probability between x_{t+1},x_t and y_t. Moreover, we define the deviation from causal independence considering the generalized Markov property $p(x_{t+1}|x_t, y_t) = p(x_{t+1}|x_t)$. When there is no causal relationship between the signals, *TE* goes do zero. In addition, *TE* is an asymmetric measure, so $TE_{Y\to X} \neq TE_{X\to Y}$ and characterizes information about x_{t+1} from the observations x_t and y_t.

The finite size and nonstationarity of EEG data introduce noise on *TE* measurement. To filter this noise, we used two additional steps that increase the measurement accuracy (Shovon *et al* 2014). These two steps consist of subtracting from $TE_{Y\to X}$ the mean value of $TE_{\tilde{Y}\to X}$, where $\tilde{Y}$ is the randomization of signal Y and normalizing this difference by the conditional entropy of x_{t+1} given x_t, as follows:

$$NTE_{Y\to X} = \frac{TE_{Y\to X} - \langle TE_{\tilde{Y}\to X}\rangle}{H(x_{t+1}|x_t)}. \quad (3)$$

where

$$H(x_{t+1}|x_t) = -\sum_{x_{t+1},x_t} p(x_{t+1}, x_t) \log_2 \frac{p(x_{t+1}, x_t)}{p(x_t)}. \quad (4)$$

Thus the ensemble of surrogates $\tilde{Y}$ avoid spurious causality information in *NTE* estimation.

Thus, the EEG signal recorded during writing-from-memory task was segmented into six windows with 20 s. For each window, we calculated the *NTE* connectivity matrix, which were averaged in a mean *NTE* connectivity matrix. This process was performed for the same EEG rhythms used in the power spectra analysis, as described in section 2.4.1.

2.4.3. Betweenness centrality

To evaluate the brain connectivity dynamics in dystonia, we used the connectivity matrix provided by the *NTE* measure (described in section 2.4.2) denoted by a_{uv}. To characterize the centrality properties of subjects' networks and provide information for hub definition, we used a measure based on the small path length concept, called betweenness centrality (BC). Small path length concept is defined by $d_{kj} = \sum_{a_{uv}\in g_{k\leftrightarrow j}} a_{uv}$, where $g_{k\leftrightarrow j}$ is the small path length between the nodes k and j (Rubinov and Sporns 2010). From this concept, BC is the fraction of all small path length that a given node participates, expressed by:

$$B_i = \frac{1}{(n-1)(n-2)} \sum_{k\in N}\sum_{j\in N} \frac{\#d_{kij}}{\#d_{kj}}, \quad \text{for } k\neq i,\ k\neq j \text{ and } j\neq i, \quad (5)$$

where $\#d_{kj}$ is the number of shortest paths between k and j, and $\#d_{kij}$ is the number of shortest paths between k and j that pass through i.

2.4.4. Hubs

To define the hubs in the network, we used a method proposed by da Silva *et al* (2017) and used by Arruda Baltazar *et al* (2019), which uses a left-sided Mann–Whitney test to compare the B_i value of one node

with all remaining nodes considering a significance level of 0.05. The node that has a B_i statistically higher than all remaining nodes is called hub and allocated in a set called connective core network, denoted by $\mathcal{B}$. van den Heuvel and Sporns (2013) describes the connective core as a substructure composed by hub regions that are densely interconnected and promote efficient communication and functional integration. In this way, the average $\Gamma_{\mathcal{B}}$ of the betweenness values from the set $\mathcal{B}$ provides a contribution measure of the hubs to the effective connectivity of the brain network.

2.4.5. Microstates

To investigate the emergent topography patterns from the EEG data, we applied the analysis of MS for all tasks. This analysis defines spatial distribution from electric potential over time from multivariate EEG signal. This analysis is supported by the global field potential (*GFP*) function defined by:

$$GFP(t) = \sqrt{\frac{\sum_{n}^{i=1}(\mathrm{EEG}_i(t) - \overline{\mathrm{EEG}(t)})^2}{n}}, \qquad (6)$$

where $\mathrm{EEG}_i(t)$ is the electric potential of the channel i at time t, $\overline{\mathrm{EEG}}(t)$ is the mean electric potential of all channels at time t, and n is the quantity of EEG channels. From the *GFP* signal, four MS can be characterized and correlated with neuroimaging findings (Michel and Koenig 2018): auditory, visual, default mode network (DMN) and attentional. In addition, we can calculate metrics that will characterize each microstate: (i) average duration of a given microstate in milliseconds (*ms*); (ii) frequency of occurrence of a microstate in the period of one second; and (iii) coverage, which consists of the percentage of the *GFP* that is represented by a given microstate.

In this work, the microstate analysis was performed in Microstate EEGlab Toolbox (available for MATLAB). The tasks performed in this study provides spontaneous EEG data, and we needed to run a highpass filter of 30 Hz and a lowpass filter of 1 Hz to compute MS (Poulsen *et al* 2018).

2.4.6. Behavioral data analysis

To evaluate the performance of the subjects during the motor tasks (described in section 2.1), we considered the average number of beats per block for the finger-tapping, that is, whenever the volunteer touched his thumb on any other finger, a beat was counted; and for the performance during the writing-from-memory, the average number of words written per block was quantified.

2.4.7. Statistical analysis

For the comparative analysis of data from the same subject, we used the Wilcoxon nonparametric W-test for paired samples. For the analysis of data between independent samples, we used the non-parametric Mann–Whitney U-test. Statistical analysis was performed using the MATLAB® 2018a software (Mathworks, Massachusetts USA) considering a statistical significance level of 0.05.

3. Results

To study the brain connectivity dynamics in patients with dystonia using multivariate EEG data, our patients and healthy volunteers were submitted to motor tasks such as finger-tapping and writing-from-memory tasks (see section 2.3). From the EEG recorded during these tasks, we performed a power spectra analysis over the right and left hemispheres of sensorimotor cortex (see section 2.4.1) and we applied the normalized transfer entropy (*NTE*, described in section 2.4.2) to infer the brain connectivity, and then assess their centrality properties (see sections 2.4.3 and 2.4.4). In addition, we also evaluated the functional networks of dystonia using MS analysis (see section 2.4.5). During the writing task all patients presented dystonic posture, characterized either by sustained extension or flexion of the wrist and a tight grip of the pen. During the finger-tapping task, only seven patients presented dystonic posture, and those were the patients with the highest scores on the Burke-Fahn-Marsden dystonia rating scale (supplemental material, table S1).

When we evaluated the performance of patients and healthy volunteers in the motor tasks, the patients with dystonia had a worse performance than the healthy volunteers when we considered the number of beats per block during the finger-tapping task (controls 57.45 and patients 49.6; $W = 336$, $p_W = 0.046$), as well as during the writing-from-memory task, considering the number of written words per block (controls 10.63 and patients 6.64; $W = 277.5$, $p_W = 0.0003$).

From these results, we investigated the electrophysiological signatures in the sensorimotor cortex using the power spectra analysis. No differences were found when we compared the power spectra of $\overline{E}_{\mu}$ and $\overline{E}_{\gamma}$, from mu and gamma rhythms respectively, between the hemispheres in both groups. Moreover, no difference were observed between the hemispheres of patients and controls during all tasks. However, an event related desynchronization in the sensory-motor cortex of controls was evidenced by a difference in the power of beta-rhythm ($\overline{E}_{\beta}$) during the writing-from-memory task, with attenuation of the β-rhythm in the left hemisphere (left-hemisphere $\overline{E}_{\beta} = 0.7534$ and right-hemisphere $\overline{E}_{\beta} = 0.8231$; $U = 48$, $p_U = 0.0333$), as shown in figure 3. No differences were found in any of the tasks in the patients' group.

Moreover, using the connective core properties to evaluate the brain connectivity networks of both groups for each brain rhythm, we observed that the

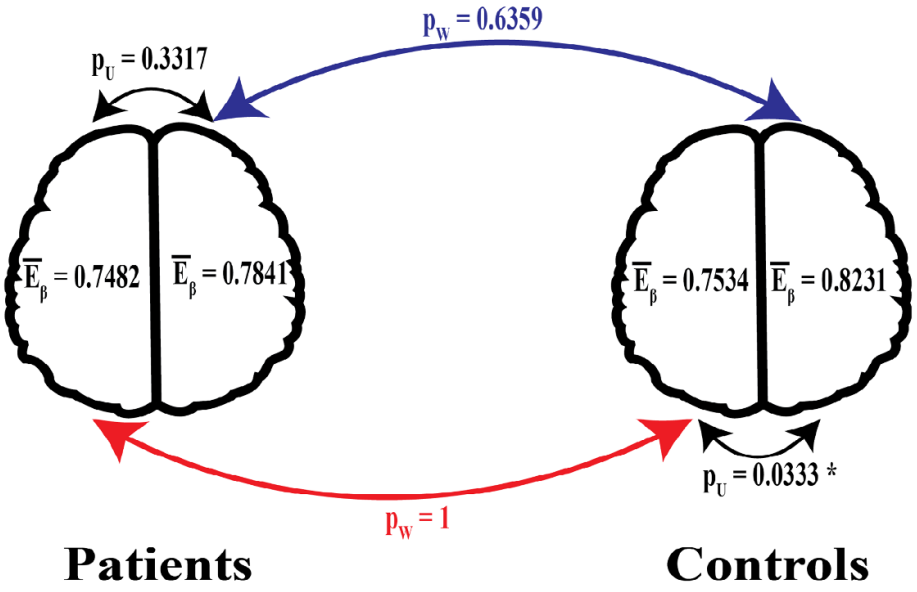

Figure 3. Comparison of power of beta-rhythm $\overline{E}_\beta$ during the writing-from-memory task. Statically significant differences were found when we compared the left-hemisphere $\overline{E}_\beta = 0.7534$ and right-hemisphere $\overline{E}_\beta = 0.8231$ ($U = 48$, $p_U = 0.0333$) in the control group. This finding was not observed in the dystonia group.

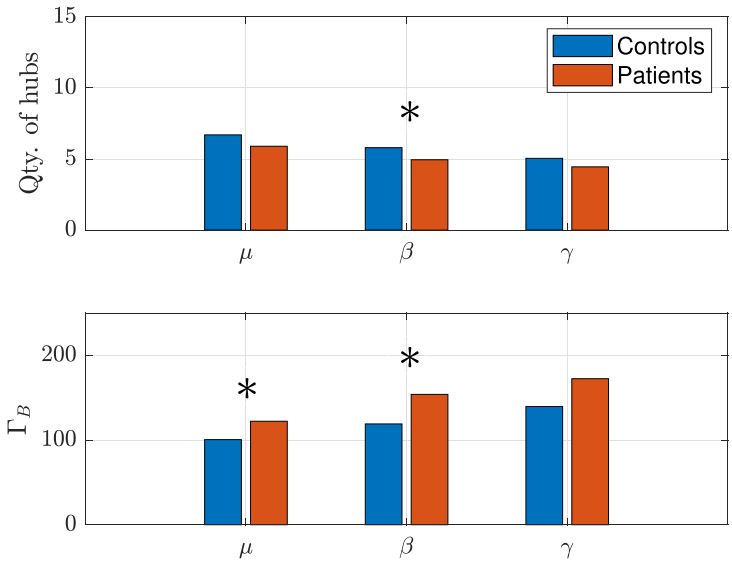

Figure 4. Comparison of hubs' quantity and contribution ($\Gamma_\mathcal{B}$) between groups during the writing-from-memory task. Statically significant differences were found in the number of hubs ($W = 483.5$, $p_W = 0.0423$) for β-rhythm and in the $\Gamma_\mathcal{B}$ measure between patients and controls at μ-rhythm ($W = 324$, $p_W = 0.0207$) and at β-rhythm ($W = 289$, $p_W = 0.0110$).

patients' group have a higher hubs' contribution ($\Gamma_\mathcal{B}$) than controls in the μ-rhythm (controls $\Gamma_\mathcal{B} = 100.51$ and patients $\Gamma_\mathcal{B} = 122.22$; $W = 324$, $p_W = 0.0207$) and in the β-rhythm (controls $\Gamma_\mathcal{B} = 119.04$ and patients $\Gamma_\mathcal{B} = 153.94$; $W = 289$, $p_W = 0.0110$). In addition, our results show that although patients have a higher contribution in the effective connectivity, their number of nodes composing the connective core in the β-rhythm is significantly lower than controls (5.8 hubs in controls and 4.9 hubs in patients; $W = 483.5$, $p_W = 0.0423$), as shown in figure 4. The number of surrogates used in the *NTE* estimation was 30.

The *NTE* provides us a quantification of the effective connectivity, to analyze the functional connectivity properties of brain networks. We used the MS analysis to characterize topographic patterns that might emerge from cortex, as auditory, visual, attentional and DMNs. From these patterns, its possible to extract measures as: coverage, duration and occurrence. No differences were found between groups regardless the task or the measure. However, during resting-state, the patients presented a DMN's microstate duration lower than controls (control DMN-duration 90.79 ms and patient DMN-duration 85.51; $W = 492$, $p_W = 0.0272$), as represented in figure 5.

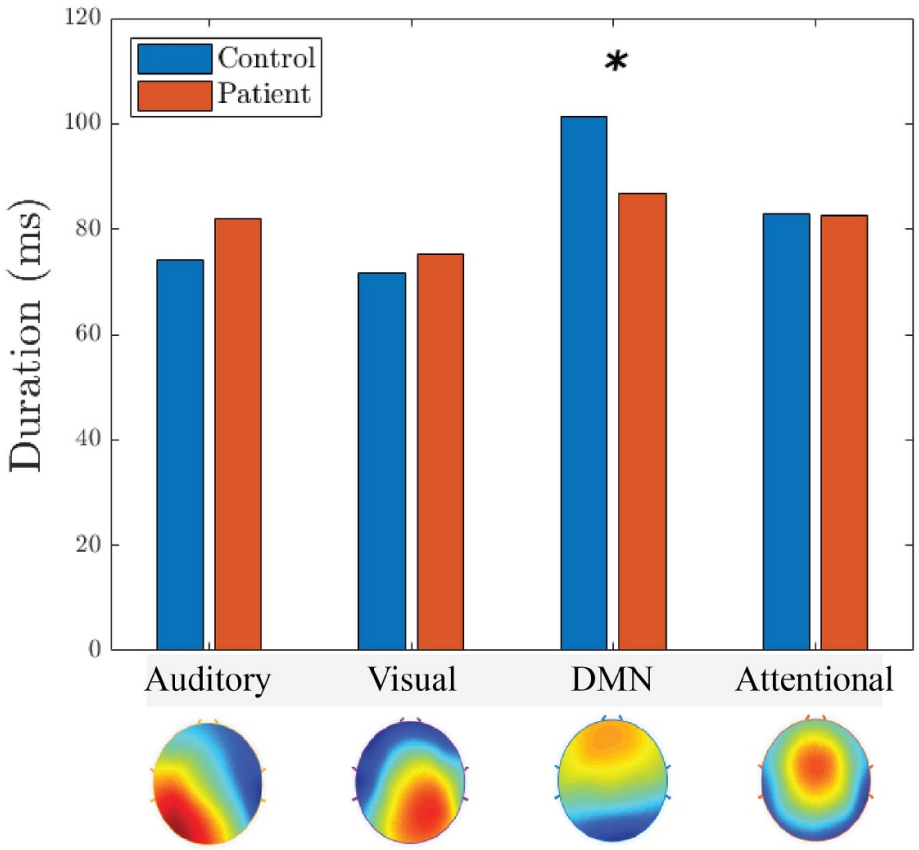

Figure 5. Comparison of microstates' duration between groups during the resting-state. The patients presented a default-mode-network microstate duration lower than controls ($W = 492$, $p_W = 0.0272$).

Finally, we applied a multi-linear regression (due to the sample size) to verify the predictability of the subjects' performance—mean number of beats per block during the finger-tapping task ($\overline{N}_b$) and the mean number of written words per block during the writing-from-memory task ($\overline{N}_w$) – considering the spectral signatures, connectivity patterns and MS. This analysis was performed assessing the linear matrix coefficients ρ from the equation $\boldsymbol{Y} = \boldsymbol{X}\rho + \epsilon$, where $\boldsymbol{Y}$ is a matrix composed by the performance scores for each subject and $\boldsymbol{X}$is a matrix composed by the power of β-rhythm for left and right brain hemispheres ($\overline{E}_{\beta,\text{left}}$ and $\overline{E}_{\beta,\text{right}}$), the hubs' contribution in μ and β rhythms ($\Gamma^{\mu}_{\mathcal{B}}$ and $\Gamma^{\beta}_{\mathcal{B}}$), the number of hubs from β-rhythm ($N^{\beta}_{\mathcal{B}}$) and the DMN's microstate time duration (T_{DMN}). In this context, ε denotes the residual error from the difference between the predicted values $\hat{\boldsymbol{Y}}$ and the real values $\boldsymbol{Y}$. The linear system obtained was:

$$\begin{aligned}\hat{\overline{N}}_b = {} & 50.6384(0.0696) + 10.0136(0.6774)\ \overline{E}_{\beta,\text{left}} \\ & - 18.7438(0.3526)\ \overline{E}_{\beta,\text{right}} - 0.0517(0.4736)\ \Gamma^{\mu}_{\mathcal{B}} \\ & + 0.0240(0.7753)\ \Gamma^{\beta}_{\mathcal{B}} + 1.7040(0.5454)\ N^{\beta}_{\mathcal{B}} \\ & + 0.0395(0.6960)\ T_{\text{DMN}} + \epsilon\ (R^2 = 0.1008)\ ,\end{aligned} \tag{7}$$

$$\begin{aligned}\hat{\overline{N}}_w = {} & 1.2795(0.8487) - 0.8550(0.8854)\ \overline{E}_{\beta,\text{left}} \\ & - 0.5602(0.9097)\ \overline{E}_{\beta,\text{right}} \\ & + 0.0165(0.3558)\ \Gamma^{\mu}_{\mathcal{B}} - 0.0058(0.7793)\ \Gamma^{\beta}_{\mathcal{B}} \\ & + 0.4089(0.5564)\ N^{\beta}_{\mathcal{B}} + 0.0571(0.0274)\ T_{\text{DMN}} \\ & + \epsilon\ (R^2 = 0.2428)\ .\end{aligned} \tag{8}$$

The p-values for the linear coefficient tests are contained inside the brackets in both equations. We observed that the time duration of DMN's microstate during resting-state task can be considered as a predictable variable for the mean number of written words per block, as seen in equation (8). However, it is important to note that the variance explainability of these models was very low for the two performance scores.

4. Discussion

Dystonia pathophysiology is highly complex. Several studies point to a loss of inhibition, abnormalities of sensorimotor integration and maladaptive neuroplasticity as key elements of this disorder, but there is a knowledge gap on how these different mechanisms are interacting (Hallett 2006, Quartarone and

Pisani 2011, Altenmüller *et al* 2012). the concept of dystonia as network disorder provides new insights into the dynamics of information flow between different regions involved in motor control (Neychev *et al* 2011, Schirinzi *et al* 2018).

In the present study, we worked with a highly selected group of patients with focal upper limb dystonia, in order to avoid confounding effects that could result from multiple motor components present in other forms of dystonia. It is well established that μ, β and γ-rhythms are associated with the cortical processing of motor control, therefore we chose to analyze them during motor tasks (Pfurtscheller *et al* 1994).

Although no differences were found in the μ and γ-rhythm, during the writing task, the analysis of $\overline{E}_{\beta}$ showed a difference between hemispheres in the control group, where the β-rhythm was attenuated in the cortex contralateral to the movement, within the expected physiological patterns (see McFarland *et al* (2000)). However, in dystonia patients, beta ERD was not observed during the motor tasks, suggesting a failure in the intracortical inhibition mechanisms. It is well established that intracortical inhibition mechanisms play a relevant role to adjust and perform a selective execution of desired movements (Denny-Brown 1967) and the basal nuclei are widely involved in these mechanisms, modulating cortical activity through the direct and indirect pathways (Beck and Hallett 2011). Therefore, this alteration of β-rhythm may be the cortical effect of the imbalance between these pathways that modulate movement, thus corroborating the hypothesis of changes in excitability and/or decrease in cortical inhibition proposed by the present work. Furthermore, this finding is in agreement with other studies (Toro *et al* 2000, Kristeva *et al* 2005), who also described alterations in ERD effects in the motor cortex contralateral to the movement in the patients with writer's cramp. Both studies reported a decrease in the desynchronization of β-rhythm in patients with writer's cramp. Toro *et al* (2000) associate this effect to dysfunction in the motor cortex, possibly as a consequence of of abnormal basal ganglia input, which is consistent with the dystonia's pathophysiology. Kristeva *et al* (2005), however, found β-rhythm differences in both contralateral and ipsilateral motor cortices of patients, associating these effects to an impairment of sensorimotor integration during preparation and execution of movements. In other movement disorders, such as Parkinson's disease (PD), broad beta oscillations are characteristic, both in cortical and subcortical areas. Some studies reported a smaller decrease of β-power prior and during movement than controls, similar to our findings in dystonia, where no decrease was observed (Heinrichs-Graham *et al* 2014), whereas an increase in the β-power during the preparatory phase preceding a speech task has been observed (Sörös *et al* 2017). Dystonia is a hyperkinetic movement disorder, and failure of intracortical inhibition mechanisms account for its pathophysiology. Although PD is considered as a classical hypokinetic disorder, it also has marked hyperkinetic features, such as tremor. In PD, an increase (or lack of decrease) of β-power in the motor cortex could be reflecting a lack of initiation of new motor plans, typical of hypokinetic movement disorders.

To better detail the previous findings, we analyzed the effective connectivity aspects of both groups during the writing task using the concept of complex networks to extract indicators that would provide information about the brain connectivity for each rhythm. We selected two measures: the number of hubs and the average contribution of this set ($\Gamma_{\mathcal{B}}$). In the γ-rhythm there were no differences between groups. However, for the μ and β rhythms, patients presented more intense hubs than the controls. Moreover, considering only the β-rhythm, they also exhibited a smaller number of hubs than the controls. These findings diverge from the results found by Battistella *et al* (2015) using MRI, but they are in agreement with the concepts of overload and failure of hubs in neurological diseases proposed by Stam (2014). Battistella *et al* (2015) describe a loss of the normal hemispheric asymmetry in patients, characterized by the measurement of modularity and a lower intensity in the information flow in the brain networks between the basal nuclei and the cerebellum, quantified by the intensity of the hubs. Our study has methodological differences when compared to Battistella's work, which includes different types of dystonia. In this way, functional magnetic resonance connectivity studies can provide a sufficiently large set of cortical and subcortical nodes to analyze modularity parameters and, although this is not possible with a set of thirty-two channels EEG, we were able to find abnormalities in patients' core networks. Stam (2014) argues that a cycle of overloading followed by failure of nodes with such expressive centrality can lead to a cascade of failures that, in turn, hamper the network's functional integration and segregation mechanisms at such a level that its resilience cannot withstand. He also describes this same behavior in neurological diseases such as epilepsy, multiple sclerosis, and Alzheimer's disease. The results of the present work, in the β-rhythm, suggest the same type of pathological signature described by Stam (2014), in which the patients have a deficient and overloaded connective core when compared to controls, thus evidencing the existence of topological changes in the cortical connectivity network. However, the fact that there are no differences between groups regarding the size of the core network, but rather a higher mean intensity of hubs in the patients, suggests that this is a functional consequence of the effect found in β.

Although the EEG data offer precise temporal information allowing to detect many brain dynamics emergent phenomena, it cannot provide any

information about subcortical structures. MS analysis makes it possible to map functional networks from EEG data that can be compared to those obtained from other methods which might access subcortical structures. With microstate analysis during resting-state, writing-from-memory and finger-tapping tasks, we found significant differences only in duration measure of DMN microstate during the resting state. In addition, as showed in multi-linear regression analysis (the equation (8)), the duration of the DMN microstate was the only measure that showed significant relationship with the prediction of subjects' performance during the writing-from-memory task. This result suggests a association of a smaller DMN microstate duration with a worst performance of patients during writing-from-memory task. The MS method is predominantly used in resting-state data; in this work, we promoted an exploratory approach using this method in motor tasks, trying to characterize any possible topographic signature of dystonia. However, this approach did not provide any biomarker during these tasks. In the work proposed by Berg *et al* (2001), they describe that the control of cognitive response of patients with writer's cramp is different to healthy individuals and that this might be related to changes in sensory input processing and motor response. Imbalances in this mechanism are traditionally associated with changes or disorganization in the somatotopic representations in the sensorimotor cortex. Although Berg *et al* (2001) did not use the microstate analysis itself and only considered event-related potential, our approach evaluates the *GFP* amplitude and the topographies present in the event-related potential data. Our findings suggest that patients' DMN MS during resting-state have a lower duration than controls'. This result is in accordance with an fMRI study conducted by Mohammadi *et al* (2012), describing differences in the resting-state DMN connectivity in patients with writer's cramp. They found increased connectivity between the left putamen and DMN, this result may reflect dysfunction of cortico-subcortical circuits in writer's cramp and reduced functional segregation of basal nuclei during resting state. Thus, the shorter duration of patients' DMN microstate can be the electrophysiological resultant of abnormal interactions between cortico-subcortical structures.

Although we can only investigate aspects of functional and effective connectivity due to limitations of the adopted methodology, the sum of these results reinforces the hypothesis of the existence of abnormalities in the connectivity of brain networks in patients with dystonia.

5. Conclusion

In this work we analyzed the brain connectivity patterns of upper limb dystonia across three tasks: resting-state, writing-from-memory and finger-tapping. Thus, using power spectral analysis, we observed that patients did not show the expected ERD during writing-from-memory task, suggesting a disruption of intracortical inhibition mechanisms. For this task, our findings also indicated a deficient and overloaded core network, similar to what is usually seen in other neurological disorders such as Alzheimer's disease (de Haan *et al* 2012) and PD (Koshimori *et al* 2016). Differences in patients' resting-state DMN MS may indicate an electrophysiological signature of abnormalities in resting functional networks and have a predictive relation with patients' performance. Overall, these findings provided information about the dynamics of the interaction between brain sites and corroborated with the hypothesis that focal upper limb dystonia is a network disorder.

Conflicts of interest

None of the authors who participated in the development of this work have conflicts of interest with this article.

Acknowledgments

This work was supported by Sociedade Beneficente Israelita Brasileira Albert Einstein and Associação PROUNIEMP. We thank all volunteers for participating in this study.

ORCID iDs

Carlos Arruda Baltazar https://orcid.org/0000-0002-4298-8315
Birajara Soares Machado https://orcid.org/0000-0001-7119-4170
Artur José Marques Paulo https://orcid.org/0000-0003-1623-0639

References

Albanese A *et al* 2013 Phenomenology and classification of dystonia: a consensus update *Movement Disorders* **28** 863–73
Altenmüller E, Baur V, Hofmann A, Lim V K and Jabusch H-C 2012 Musician's cramp as manifestation of maladaptive brain plasticity: arguments from instrumental differences *Ann. New York Acad. Sci.* **1252** 259–65
Aoki F, Fetz E, Shupe L, Lettich E and Ojemann G 1999 Increased gamma-range activity in human sensorimotor cortex during performance of visuomotor tasks *Clin. Neurophysiol.* **110** 524–37
Arruda Baltazar C, Barros Guinle M I, Caron C J, Amaro E and Soares Machado B 2019 Connective core structures in cognitive networks: The role of hubs *Entropy* **21** 961
Babiloni C *et al* 2016 Alpha, beta and gamma electrocorticographic rhythms in somatosensory, motor, premotor and prefrontal cortical areas differ in movement execution and observation in humans *Clin. Neurophysiol.* **127** 641–54
Battistella G, Termsarasab P, Ramdhani R A, Fuertinger S and Simonyan K 2015 Isolated focal dystonia as a disorder of

large-scale functional networks *Cerebral Cortex* **27** bhv313

Beck S and Hallett M 2011 Surround inhibition in the motor system *Experimental Brain Res.* **210** 165–72

Berg D, Herrmann M, Müller T J, Strik W, Aranda D, König T, Naumann M and Fallgatter A 2001 Cognitive response control in writer's cramp *Eur. J. Neurology* **8** 587–94

da Silva L M U, Baltazar C A, Silva C A, Ribeiro M W, de Aratanha M A A, Deolindo C S, Rodrigues A C and Machado B S 2017 Measures for brain connectivity analysis: nodes centrality and their invariant patterns *Eur Phys. J. Special Topics* **226** 2235–45

Damoiseaux J S, Rombouts S, Barkhof F, Scheltens P, Stam C J, Smith S M and Beckmann C F 2006 Consistent resting-state networks across healthy subjects *Proc. Natl Acad. Sci.* **103** 13848–53

de Haan W, Mott K, van Straaten E C, Scheltens P and Stam C J 2012 Activity dependent degeneration explains hub vulnerability in alzheimer's disease *PLoS Computat. Biol.* **8** e1002582

Denny-Brown D 1967 The fundamental organization of motor behavior *Neurophysiological Basis of Normal and Abnormal Motor Acrioities* pp 415–42

Dresel C, Li Y, Wilzeck V, Castrop F, Zimmer C and Haslinger B 2014 Multiple changes of functional connectivity between sensorimotor areas in focal hand dystonia *J. Neurol. Neurosurg. Psychiatry.* **85** 1245–52

Fahn S, Bressman S B and Marsden C D 1998 Classification of dystonia *Adv. Neurol.* **78** 1–10

Freeman S M, Itthipuripat S and Aron A R 2016 High working memory load increases intracortical inhibition in primary motor cortex and diminishes the motor affordance effect *J. Neurosci.* **36** 5544–55

Friston K J 2011 Functional and effective connectivity: a review *Brain Connectivity* **1** 13–36

Gallea C *et al* 2015 Increased cortico-striatal connectivity during motor practice contributes to the consolidation of motor memory in writer's cramp patients *NeuroImage: Clinical* **8** 180–92

Hallett M 2006 Pathophysiology of dystonia *Parkinson's Disease and Related Disorders* (Berlin: Springer) pp 485–8

Heinrichs-Graham E *et al* 2014 Neuromagnetic evidence of abnormal movement-related beta desynchronization in parkinson's disease *Cerebral Cortex* **24** 2669–78

Jasper H and Penfield W 1949 Electrocorticograms in man: effect of voluntary movement upon the electrical activity of the precentral gyrus *Archiv für Psychiatrie und Nervenkrankheiten* **183** 163–74

Jeong J 2004 Eeg dynamics in patients with alzheimer's disease *Clin. Neurophysiol.* **115** 1490–505

Jin S-H, Lin P and Hallett M 2011 Abnormal reorganization of functional cortical small-world networks in focal hand dystonia *PloS One* **6** e28682

Koch M A, Norris D G and Hund-Georgiadis M 2002 An investigation of functional and anatomical connectivity using magnetic resonance imaging *Neuroimage* **16** 241–50

Koshimori Y *et al* 2016 Disrupted nodal and hub organization account for brain network abnormalities in parkinson's disease *Front. Aging Neurosci.* **8** 259

Kristeva R, Chakarov V, Losch F, Hummel S, Popa T and Schulte-Mönting J 2005 Electroencephalographic spectral power in writer's cramp patients: evidence for motor cortex malfunctioning during the cramp *Neuroimage* **27** 706–714.

Lo C-Y, Wang P-N, Chou K-H, Wang J, He Y and Lin C-P 2010 Diffusion tensor tractography reveals abnormal topological organization in structural cortical networks in alzheimer's disease *J. Neurosci.* **30** 16876–85

Machado B S, Kunicki A C B, Morya E and Sameshima K 2012 Spectral characteristics of the hippocampal lfp during contextual fear conditioning *Einstein (Sao Paulo)* **10** 140–4

McFarland D J, Miner L A, Vaughan T M and Wolpaw J R 2000 Mu and beta rhythm topographies during motor imagery and actual movements *Brain Topography* **12** 177–86

Michel C M and Koenig T 2018 Eeg microstates as a tool for studying the temporal dynamics of whole-brain neuronal networks: a review *Neuroimage* **180** 577–93

Mohammadi B, Kollewe K, Samii A, Beckmann C F, Dengler R and Münte T F 2012 Changes in resting-state brain networks in writer's cramp *Human Brain Mapping* **33** 840–8

Neychev V K, Gross R E, Lehéricy S, Hess E J and Jinnah H 2011 The functional neuroanatomy of dystonia *Neurobiol. Dis.* **42** 185–201

Pfurtscheller G, Brunner C, Schlögl A and Da Silva F L 2006 Mu rhythm (de) synchronization and eeg single-trial classification of different motor imagery tasks *NeuroImage* **31** 153–9

Pfurtscheller G, Pregenzer M and Neuper C 1994 Visualization of sensorimotor areas involved in preparation for hand movement based on classification of μ and central β rhythms in single eeg trials in man *Neurosci. Lett.* **181** 43–6

Poulsen A, Pedroni A, Langer N and Hansen L 2018 Microstate eeglab toolbox: An introductory guide

Quartarone A and Pisani A 2011 Abnormal plasticity in dystonia: disruption of synaptic homeostasis *Neurobiol. Dis.* **42** 162–70

Rubinov M and Sporns O 2010 Complex network measures of brain connectivity: uses and interpretations *Neuroimage* **52** 1059–69

Sörös P, Doñamayor N, Wittke C, Al-Khaled M, Brüggemann N and Münte T F 2017 Increase in beta-band activity during preparation for overt speech in patients with parkinson's disease *Front. Human Neurosci.* **11** 371

Schirinzi T, Sciamanna G, Mercuri N B and Pisani A 2018 Dystonia as a network disorder: a concept in evolution *Curr. Opinion Neurol.* **31** 498–503

Schreiber T 2000 Measuring information transfer *Phys. Rev. Lett.* **85** 461

Shovon M H I, Nandagopal D N, Vijayalakshmi R, Du J T and Cocks B, 2014 Transfer entropy and information flow patterns in functional brain networks during cognitive activity *Int. Conf. on Neural Information Processing* pp 1–10

Sporns O 2011 The human connectome: a complex network *Ann. New York Acad. Sci.* **1224** 109–25

Stam C J 2014 Modern network science of neurological disorders *Nat. Rev. Neurosci.* **15** 683

Toro C, Deuschl G and Hallett M 2000 Movement-related electroencephalographic desynchronization in patients with hand cramps: evidence for motor cortical involvement in focal dystonia *Ann. Neurology: Official J. Am. Neurolo. Association Child Neurol. Soc.* **47** 456–61

van den Heuvel M P and Sporns O 2013 Network hubs in the human brain *Trends Cognitive Sci.* **17** 683–96

Welch P 1967 The use of fast fourier transform for the estimation of power spectra: a method based on time averaging over short, modified periodograms *IEEE Trans. Audio Electroacoust.* **15** 70–3

Witt S T, Laird A R and Meyerand M E 2008 Functional neuroimaging correlates of finger-tapping task variations: an ale meta-analysis *Neuroimage* **42** 343–56

Zhao L and He Y 2013 Power spectrum estimation of the Welch method based on imagery EEG *Appl. Mech. Mater.* **278–80** 1260–4

Zoons E, Booij J, Nederveen A J, Dijk J and Tijssen M 2011 Structural, functional and molecular imaging of the brain in primary focal dystonia-a review *Neuroimage* **56** 1011–20